Ribeiro-Rodrigues Alecrim, L.; Ferreira, J.; Gutiérrez-González, C.; Salvador Moya, MD.; Borrell Tomás, MA.; Pallone, E. (2017). Effect of reinforcement NbC phase on the mechanical properties of Al2O3-NbC nanocomposites obtained by spark plasma sintering. International Journal of Refractory Metals and Hard Materials. 64:255-260. doi:10.1016/j.ijrmhm.2016.10.021

Effect of reinforcement NbC phase on the mechanical properties of Al_2O_3-NbC nanocomposites obtained by spark plasma sintering

L.R.R. Alecrim[1,3]*, J.A. Ferreira[1], C.F. Gutiérrez-González[2], M.D. Salvador[3], A. Borrell[3], E.M.J.A. Pallone[1]

[1]Universidade de São Paulo/Faculdade de Zootecnia e Engenharia de Alimentos; Av. Duque de Caxias Norte, 225, 13635-900 Pirassununga-SP, Brazil

[2]Centro de Investigación en Nanomateriales y Nanotecnología (Consejo Superior de Investigaciones Científicas, Universidad de Oviedo, Principado de Asturias), Avenida de la Vega 4-6, 33940 El Entrego, Spain

[3]Instituto de Tecnología de Materiales (ITM), Universitat Politècnica de València, Camino de Vera s/n, 46022 Valencia, Spain

*Corresponding author: Universidade de São Paulo, Av. Duque de Caxias Norte, 225, 13635-900 Pirassununga-SP, Brazil. Tel.: +34 963876230; Fax: +34 963877629
E-mail: laisribeiro@usp.br (L.R.R. Alecrim)

ABSTRACT

The sintering behavior of Al_2O_3-NbC nanocomposites fabricated via conventional and spark plasma sintering (SPS) was investigated. The nanometric powders of NbC were prepared by reactive high-energy milling, deagglomerated, leached with acid, added to the Al_2O_3 matrix in the proportion of 5 vol.% and dried under airflow. Then, the nanocomposite powders were densified at different temperatures, 1450-1600 °C. Effect of sintering temperature on the microstructure and mechanical properties such as hardness, toughness and bending strength were analyzed. The Al_2O_3-NbC nanocomposites obtained by SPS show full density and maximum hardness value >25 GPa and bending strength of 532 MPa at 1500 ºC. Microstructure observations indicate that NbC nanoparticles are dispersed homogeneously within Al_2O_3 matrix and limit their grain growth. Scanning electron microscopy examination of the fracture surfaces of dense samples obtained at 1600 ºC by SPS revealed partial melting of the particle surfaces due to the discharge effect.

Keywords: Nanocomposite; Al_2O_3-NbC; Spark Plasma Sintering; Mechanical properties; Microstructure

1. Introduction

Al_2O_3-reinforced with nano-sized particles, such as TiB_2, SiC, TiC, WC, NbC and others, represent a new class of materials with improved mechanical properties, especially the fracture toughness, hardness and wear resistance [1-9]. This new class of materials can be an interesting alternative for the production of cutting tools in order to improve cutting speed and productivity.

The carbides of transition metals are one of the most promising ceramic materials in the preparation of ceramic composites, because the chemical bonds established give specific properties to these materials. The niobium carbide shows properties that can be compared to other refractory carbides used in obtaining hard metal. It has a high melting point, high hardness and toughness and low chemical reactivity [7,8]. The advantage of use NbC as reinforcement of Al_2O_3 is that both materials have a similar thermal expansion coefficient and reducing the residual stresses produced during the heating and cooling processes, which can lead to the formation of cracks in brittle materials, causing a decrease of the strength values. Thus, Al_2O_3 and NbC are thermo-mechanically compatible.

There are various synthesis methods for producing nanometric powder for preparation new and best nanostructured materials. The reactive milling is an alternative synthesis process in which high-energy milling promotes the reaction in a mixture of reactive powders [10,11]. The advantage of this process has allowed the synthesis of powder cermets in a short time with nanometric characteristics, good stoichiometric control and low energetic cost [11]. But a disadvantage is that the high temperature reached in the reaction, causes agglomeration of particles, therefore, the deagglomeration of the powder after synthesis is necessary [12].

Recent works published in the literature have shown the potential of the use of NbC as grain growth inhibitor in WC-Co hard metals [13] and as hardening reinforcing material in ZrO_2 [9]. This suggests that the use of niobium carbide as a potential reinforcing material deserves to be further investigated.

Acchar et al. [6] obtained Al_2O_3-NbC composites from Al_2O_3 and NbC powders by pressureless sintering or hot pressing without sintering additives. With the use of 5 vol.% of NbC they obtained dense Al_2O_3-NbC composites by hot-pressed at relatively

higher temperatures (1650 ºC) and with a hardness value of 16.5 GPa. By uniaxial pressing only reached 92% of density and 13 GPa of hardness. Pallone et al. [14] obtained Al_2O_3+5wt% NbC (2.6vol.% NbC) nanocomposites by pressureless sintering at 1450 and 1500 ºC with 96 and 98% of density and 17 and 18 GPa of hardness, respectively. Nevertheless, sintering without additives requires rather high temperatures, which enhances the formation of thermal cracks. The use of sintering additives such as Y_2O_3, TiO_2 and MnO allow produce dense Al_2O_3-NbC composites via liquid-phase mechanism at relatively lower temperatures than those characteristic of the pressure-assisted processes but with similar mechanical properties [15].

To improve the sinterability of these materials and obtain mechanical and wear properties with a higher quality than the current properties, an interesting technique is the Spark plasma sintering (SPS), also known as field-assisted sintering technique (FAST). This technique is based on applying an on-off dc (direct current) electric pulse under uniaxial pressure that it is used for rapid fabrication of nanocrystalline ceramics [3,4,5]. This technique can work at heating rates on the order of hundreds of degrees per minute, reaching high temperatures in very short time, providing dense materials after cycles of heating/cooling of only a few minutes. Currently, there is an increasing interest in the sintering of oxides and non-oxides powders and hard metals by SPS [16,17]. This is especially important in the case of hard metals, because of the great significance of processing these materials at low temperatures for different fields of materials engineering.

Therefore, in this work, Al_2O_3-NbC nanocomposite powders with 5vol.% of NbC were prepared via reactive milling and sintered without additives using spark plasma sintering technique (SPS) in order to consider these materials for suitable application in the industry. The mechanical properties and microstructure of Al_2O_3-NbC nanocomposites were investigated and discussed in detail.

2. Experimental details

2.1. Preparation of the powder

The nanometric powders of alumina (Al_2O_3) and niobium carbide (NbC) were obtained by reactive high-energy milling as described in a previous work [14,18]. High-energy ball milling of the reactant powder mixtures of Al-Nb_2O_5-C-Al_2O_3 were

carried out using commercial powders of aluminum (ALCOA, 99.7% of purity), Nb_2O_5 (CBMM, 98.5% of purity), Al_2O_3 (AKP-53, Sumitomo, 99.95% of purity) and carbon black. The reaction, without the Al_2O_3 added as diluent, is given by:

$$10/3Al + Nb_2O_5 + 2C \rightarrow 5/3\ Al_2O_3 + 2NbC \quad (1)$$

The milling equipment was a Shaker Mix type, SPEX 8000, with vial and milling balls made of hardened steel. The material to ball mass ratio was fixed in 5:1, using five balls with 11 mm in diameter. The ignition time of the reaction was the 190 min and grinding was performed for 330 min for reduced the crystallite size in nanometric dimensions. After synthesis, the powders were leached in hydrochloric acid for removal of iron coming from the vial and grinding media and deagglomerated in a planetary mill (Fritsch mill) as described in a previous work [19]. The final compositions of the samples, with 5 vol.% of NbC, were obtained by adding alumina to the reactive milling products. The composite mixtures were obtained in a conventional ball mill in alcohol suspension with 0.2 wt% of PABA, 100 ppm of magnesium chloride hexahydrate ($MgCl_2.6H_2O$) and 0.5 wt% of oleic acid.

2.2. Sintering procedures

Before the conventional sintering, the powders were dried, sieve until 80 μm and isostatically pressed at 200 MPa. Conventional sintering was carried out in high vacuum at different temperatures (1550 and 1600 ºC) using a heating rate of 10 ºC/min with 60 min of dwelling time at the maximum temperature. A second set of powder was introduced into a 20-mm-diameter graphite die and sintered using an spark plasma sintering (SPS) apparatus HP D25/1 (FCT Systeme GmbH, Rauenstein, Germany) at temperatures from 1450-1600 ºC and 80 MPa of pressure to obtain fully sintered bulk materials. The tests were carried out under vacuum at a heating rate of 100 ºC/min with 5 min of dwelling time at the maximum temperature.

2.3. Characterization

Phase composition of the powder after reaction was characterized by X-ray diffraction (XRD, Rigaku diffractometer, MiniFlex 600 model). The measurements

were taken in the 0-80 º range and the step size and time of reading were 0.02 º and 0.3 s, respectively. With this diffraction pattern was made of the refinement of structural parameters by the method of Rietveld to quantify the phases of Al_2O_3 and NbC, the crystallite size was determined using the width of the Bragg peak profiles at half of the maximum intensity, according to Sheerer method [20]. The particle size was measure using HORIBA LA-950 V2 equip.

The density of the samples was measured by the Archimedes method (ASTM C373-88). Relative densities were estimated in accordance with the real density of the powder measured by Helium picnometry (4.10 g/cm^3).

Sintered samples were fractured on their cross-section and were polished to 0.25 μm using SiC paper and diamond suspension. The fracture surface was analyzed by using a field emission gun scanning electron microscope (FE-SEM, HITACHI S-4800, SCSIE of the University of Valencia).

Nanomechanical properties such as hardness (H) and Young's modulus (E) of samples were analyzed by a nanoindentation technique (Model G200, MTS Company, USA). Tests were performed under maximum depth control, 1200 nm, using a Berkovich diamond tip previously calibrated of the function are an in fused silica. The contact stiffness was determined by the Continuous Stiffness Measurement technique (CSM) to calculate the profiles of hardness and elastic modulus [21]. Amplitude was programmed to 2 nm with 45 Hz frequencies. A matrix of 25 indentations was made on each sample. The Poisson's coefficient was 0.18 for all calculations considering a fully dense material.

Mechanical properties were evaluated via micro and nano-indentation techniques. K_{IC} values were studied by the cracks induced by applying loads of 20 kg for 10 s with an image analysis program, and using the equation proposed by Niihara et al. [22]. 10 measurements have been performed in each sample.

The bending strength of the samples sintered by SPS was measured by biaxial testing using the equations of Kirstein and Woolley [23], Vitman and Pukh [24], and the standard specification ASTM F394-78. All tests were obtained at room temperature using a universal testing machine (Instron 856, MA, USA) with a cross-head displacement speed of 0.002 mm/s.

3. Results and discussion

3.1. Powder characterization

Figure 1 shows the X-ray diffraction (XRD) pattern of the powder mixtures after the reaction of high-energy milling. It is observed only peaks of the reaction product, Al_2O_3 and NbC, with no peaks relating to reagents, whereas the crystallite size was equal to 9.1 and 9.7 nm, respectively.

Due to the high temperatures reached during the mechanical alloying occurs a large agglomeration of the particles of the powder resulting from the reaction forming aggregates. These aggregates were broken in the grinding mill SPEX after the reaction to obtain the powder with nanocrystalline size.

Figure 2 shows the microstructure of the powders obtained by high-energy milling before and after deagglomeration procedure in a planetary mill. It is observed in Figure 2b the reduction of the agglomerates and the nanoparticles of NbC (white spots) homogeneously dispersed in the Al_2O_3 matrix.

Another analysis to verify deagglomeration of the powder obtained was measured for particle size distribution (Figure 3). It was observed that there was an important shift in the curves, going from 10 μm (curve a) before deagglomeration in the planetary mill and after (curve b) where the diameter of the particles reaches 1 μm, approximately. This show the need to deagglomeration before of the sintering process of powders, and therefore, obtain samples with high density and thus improve mechanical properties [25-27].

3.2. Characterization of Al_2O_3-NbC nanocomposites obtained by conventional sintering

Table 1 shows the values of the relative density (% TD) and the mechanical properties of the samples sintered by conventional furnace in argon atmosphere at 1550 and 1600 ºC. It is noted that conventional sintering at both temperatures were not sufficient for obtaining high density nanocomposites of Al_2O_3 reinforced with 5 vol.% of NbC. The hardness of the materials increases with temperature and, on the contrary, the Young's modulus and toughness decreased with increase the

temperature. The improvement in toughness value of the Al_2O_3-NbC sintered at 1550 ºC is due to the high porosity which stops the crack formation and grain pull-out [28].

Table 1. Density and mechanical properties of the Al_2O_3-5vol.% NbC nanocomposites sintered by conventional method at different temperatures.

Properties	Conventional sintering temperatures (ºC)	
	1550	1600
Density (% TD)	92.2	93.6
Hardness (GPa)	21.3	23.4
Young's Modulus (GPa)	390	209
Toughness (MPa·$m^{1/2}$)	4.1	2.4

Microstructural analysis performed on the fracture surface of the conventional sintered samples is shown in Figure 4. Figure 4(a) show the sample sintered at 1550 ºC and Figure 4(b) show the samples sintered at 1600 ºC.

The microstructure displays a homogeneous distribution of niobium carbide particles within the alumina matrix, this fact It is most remarkable in the Figure 4(b) where is reveals clearly nanoparticles of NbC (white particles) embedded in the microstructure of alumina matrix. Also, it can be seen high porosity in both micrographs, while in the sample processed at 1600 ºC the porosity is a little lower. The grain size of the alumina matrix in both microstructures is several microns (~5-7 μm).

3.3. Characterization of Al_2O_3-NbC nanocomposites obtained by SPS

The Figure 5 show the piston speed and displacement as a function of sintering temperature for a Al_2O_3-5vol.% NbC sample sintered up to 1600 ºC by SPS. In this cycle, the maximum pressure (80 MPa) was applied between 1100 and 1400 ºC, which produced the compaction of the powder. Once the maximum pressure has been reached it was held up to each final temperature. After the first piston displacement, it was observed that sintering process started at 1440 ºC and the

material was completely dense at temperatures as low as 1450 ºC, approximately. All nanocomposites show values of density >99% TD.

Usually, Al_2O_3-NbC dense materials are obtained by conventional method at high temperatures (>1600 ºC) and with using additives. In this work, keeping in mind the Figure 5, four final temperatures were chosen for sintering the materials: 1450, 1500, 1550 and 1600 ºC, as the lowest temperature at which the material appears to be sintered is 1440 ºC we choose 1450 ºC as the first temperature to study. It is important to note that it was possible to reach the theoretical density without the use of additives at sintering temperatures as low as 1450 ºC, this is consequence of the optimum homogenization and distribution of the Al_2O_3 and NbC phases obtained by high-energy ball milling process and the sintering conditions applied during SPS. With this sintering technique, the material can be densified fairly quickly because of the high heating rate employed and the pressure applied during the process.

Figure 6 (a), (b), (c) and (d) shows, respectively, the FESEM micrographs of the fracture surface of 1450 ºC, 1500 ºC, 1550 ºC and (d) 1600 ºC sintered samples, where the evolution of the alumina grain size in function of the maximum sintering temperature is observed. It was possible to obtain near full density with an average grain size similar to starting powder (1 μm) for the lowest sintering temperature tested (1450 ºC). In this case, only isolated grains with larger grain size were observed. As the sintering temperature was increased, the proportion of these alumina grains increased. It was observed that the nanometric inclusions of NbC (light regions) were homogeneously dispersed by the Al_2O_3 matrix, being distributed both on grain boundaries as inside grain (inter/intragranular positioning of NbC nanoparticles, respectively). The efficient distribution of NbC nanoparticles within the whole alumina matrix, drastically reduced the alumina grain growth with very low percentage of NbC nanoparticles.

FESEM image from the fracture surface of the sample sintered at 1600 ºC (Figure 6d) revealed local melting of the NbC nanoparticles in the edges and corners of the alumina matrix. Some particle surfaces contain traces of liquid layers that were solidified while flowing. Additionally, material jets formed from liquid are visible between Al_2O_3 particles (highlighted by circle). This indicates that very high local

temperatures, above melting point of NbC, must be present during the SPS process, despite the final temperature of which was only 1600 ºC. A reasonable explanation for the experimental results would be that the strong local melting in a SPS furnace is characteristic of the spark formed between the partially melted corner (previously unmelted) and the corner/edge/surface of the opposite particle over the gap [29,30]. In the initial stage of the SPS process, an electric field in the gaps between powder particles was created and high-temperature plasmas were excited under the action of a pulse current so that it caused a discharge between adjacent particles, leading to a local high temperature on the surface of the NbC nanoparticles. If the local temperature was high enough, localized melting of the NbC nanoparticle occurred. The local temperature in this region then decreased rapidly, and a partially melted microstructure was formed between the two particles because of the quick cooling. Consequently, the locally high temperature induced by the plasma can cause the melting and evaporation of smaller particles, and would explain why only a few small particles were observed in the partially sintered microstructure. This plasma formation scenario is consistent with the direct microstructure observed in Figure 6d and the EDS analysis performed.

It is important to remark that these microstructures are unattainable by using other sintering techniques such as pressureless sintering (Figure 4). In those cases, the characteristic longer cycles certainly promote grain growth at high temperature and microstructural design is limited. SPS process is a much more versatile technique. As it is possible to obtain dense material preserving the microstructure of the starting powdered material, the additional energy provided by further increase on sintering temperature is consumed in grain growth processes leading to microstructures showing mixture of nanometric and micrometric grains or completely microstructured materials similar to those obtained by alternative techniques. Then, SPS sintering appears as a very powerful tool for microstructural design.

Table 2 shows the values of the mechanical properties of the Al_2O_3-5vol.% NbC nanocomposites sintered by SPS at different temperatures. It can be seen that the nanocomposites obtained by SPS show a high hardness values, even at lower temperatures, compared with samples obtained in this work by conventional sintering, and higher than that reported by others authors for Al_2O_3-TiC [4], Al_2O_3-

NbC [6,8,14], ZrO_2-NbC [9] and Al_2O_3-WC [31]. This increase is due to several factors: applied pressure, fast-heating rates, short dwelling times and a homogeneous microstructure, as has seen previously. These factors leads to strong ceramic bond between the interfaces of the particles as resulting in increased final properties of the material. An important result is the hardness value to the sample obtained by SPS at 1450 ºC, which is an 8% higher than sample obtained by conventional at 1600 ºC, the saving time and energy is significant. These aspects are ones of the main criteria for the selection of the material for cutting tool application.

Table 2. Mechanical properties of the Al_2O_3-5vol.% NbC nanocomposites sintered by SPS at different temperatures.

Mechanical properties	SPS temperatures (ºC)			
	1450	1500	1550	1600
Hardness (GPa)	25.4	25.2	25.1	24.4
Young's modulus (GPa)	462	454	466	444
Toughness (MPa·$m^{1/2}$)	2.9	2.8	3.0	3.5
Bending strength (MPa)	318	532	460	430

In summary, all samples, independently of the sintering temperature, showed good combination of mechanical properties. The best value of hardness was reached for the Al_2O_3-5vol.% NbC nanocomposite sintered at 1450 ºC, while maximum bending strength corresponded to sample prepared at 1500 ºC. The differences in mechanical properties are related to the evolution of the microstructures of the sample (Figure 6). As a general trend, in materials with similar densities, with increasing grain size the hardness decreases according to a Hall–Petch type relationship [32], but fracture toughness tends to increase. Bending strength values of the materials reported in literature fall within the strength range (300–350 MPa), suggesting that the type of carbide addition has no significant influence on the mechanical strength of the composite material [4,6,8,9,14,31]. The strength depends basically on the presence of defects in the microstructure such as pores, agglomerates and cracks produced by differences between the thermal expansion coefficient of the matrix and the

reinforcing carbide. Also, it is known that the binder or liquid phase in materials prevents the crack propagation by shielding the stress field in front of crack tip or by bridging the crack forming ligaments behind the crack tip [33]. Therefore, the sample sintered at 1600 ºC has a higher value of toughness than samples sintered at lower temperatures.

The samples sintered at 1450 ºC and 1500 ºC had higher proportion of submicrometric grains, <2 μm, and consequently they showed the highest hardness values and moderate fracture toughness. Nevertheless, when both samples were compared, it could be seen that nanocomposite prepared at 1500 ºC had 40% higher bending strength. Probably, the difference can be attributed, firstly, to the low residual porosity of the material sintered at the lowest temperature that acted as critical flaws and, therefore, a sample with a lower bending strength was observed.

4. Conclusions

The results obtained from characterization of pressureless sintering and spark plasma sintering Al_2O_3-5vol.% NbC nanocomposites revealed that:

- The reactive high-energy milling was effective to obtain nanometric powders of Al_2O_3-NbC with small crystallite size.
- Pressureless sintering showed low densification (92-94% TD) while by SPS is it possible to obtain fully dense nanocomposites at very low temperature 1450 ºC.
- The microstructural analysis of the nanocomposites sintered at temperatures below 1500 ºC reveals a submicron alumina grain size and homogeneous distribution of niobium carbide in the alumina matrix. This improved the hardness, reaching values >25 GPa, therefore, this result suggests the possibility of its use as cutting tools materials.
- Direct observation by FESEM in sample sintered by SPS at 1600 ºC revealed traces of local melting and material jets between particles. The high-temperature spark plasma could momentarily be generated in the gaps due to the electrical discharge effect between powder particles at the beginning of on-off dc pulse energizing.

This work presents, at the first time, Al_2O_3-NbC nanocomposites fabricated by SPS at low temperature, resulting with high density and mechanical properties compared with others conventional consolidation methods, therefore, opens a window of opportunities to fabrication new materials.

Acknowledgements

This work has been financial support by the Brazilian institution CAPES for the project CAPES-PVE A086/2013 (project Nº 23038.009604/2013-12). A. Borrell, acknowledges the Spanish Ministry of Economy and Competitiveness for her *Juan de la Cierva-Incorporación* contract (IJCI-2014-19839).

References

[1] S.C. Tjong, Z.Y. Ma, R.K.Y. Li, The dynamic mechanical response of Al_2O_3 and TiB_2 particulate reinforced aluminum matrix composites produced by in-situ reaction, Mater. Lett. 38 (1999) 39-44.

[2] D. Jianxin, A. Xing, Wear resistance of Al_2O_3/TiB_2 ceramic cutting tools in sliding wear tests and in machining processes, J. Mater. Process. Technol. 72 (1997) 249-255.

[3] A. Borrell, I. Álvarez, R. Torrecillas, V.G. Rocha, A. Fernández, Microstructural design for mechanical and electrical properties of spark plasma sintered Al_2O_3-SiC nanocomposites, Mater. Sci. Eng. A 534 (2012) 693-698.

[4] R. Kumar, A.K. Chaubey, S. Bathula, B.B. Jha, A. Dhar, Synthesis and characterization of Al_2O_3-TiC nano-composite by spark plasma sintering, Int. J. Refract. Met. Hard Mater. 54 (2016) 304-308.

[5] W.H. Chen, H.T. Lin, P.K. Nayak, M.P. Chang, J.L. Huang, Sintering behavior and mechanical properties of WC-Al_2O_3 composites prepared by spark plasma sintering (SPS), Int. J. Refract. Met. Hard Mater. 48 (2015) 414-417.

[6] W. Acchar, P. Greil, A.E. Martinelli, C.A.A. Cairo, A.H.A. Bressiani, J.C. Bressiani, Sintering behaviour of alumina-niobium carbide composites, J. Eur. Ceram. Soc. 20 (2000) 1765-1769.

[7] R.M.R. Pasoti, J.C. Bressiani, Sintering of alumina-niobium carbide composite. Int. J. Refract. Met. Hard Mat. 16 (1998) 423-427.

[8] W. Acchar, A.M. Segadães, Properties of sintered alumina reinforced with niobium carbide, Inter. J. Refract. Met. Hard Mater 27 (2009) 427-430.

[9] C. Santos, L.D. Maeda, C.A.A. Cairo, W. Acchar, Mechanical properties of hot pressed ZrO_2-NbC ceramic composites, Int. J. Refract. Met. Hard Mater. 26 (2008) 14-18.

[10] E.M.J.A. Pallone, V. Trombini, F.W.J. Botta Filho, R. Tomasi, Ceramic processing of nanometric powders obtained by reactive milling, Mater. Sci. Forum, 727-728 (2012) 909-913.

[11] K.P.S. Tonello, V. Trombini, A.H.A. Bressiani, J.C. Bressiani, Ceramic processing of NbC nanometric powders obtained by high energy milling and by reactive milling, Mater. Sci. Forum, 403 (2002) 65-70.

[12] R.E. Kahrizsangi, M. Abdellahl, M. Bahmanpour, Self-ignited synthesis of nanocomposite powders induced by Spex mills; modeling and optimizing, Ceram. Inter. 41 (2015) 3137-3151.

[13] S.G. Huang, R.L. Liu, L. Li, O. Van der Biest, J. Vleugels, NbC as grain growth inhibitor and carbide in WC-Co hard metals, Int. J. Refract. Met. Hard Mater. 26 (5) (2008) 389-395.

[14] E.M.J.A. Pallone, V. Trombini, F.W.J. Botta Filho, R. Tomasi, Synthesis of Al_2O_3-NbC by reactive milling and production of nanocomposites, J. Mat. Proc. Tech. 143-144 (2003) 185-190.

[15] W. Acchar, D. Schwarze, P. Greil, Sintering of Al_2O_3-NbC composites using TiO_2 and MnO additives: preliminary results, Mater. Sci. Eng. A 351 (2003) 299-303.

[16] A. Borrell, A. Fernandez, R. Torrecillas, J.M. Cordoba, M.A. Aviles, F.J. Gotor, Spark plasma sintering of ultrafine TiC_xN_{1-x} powders synthesized by a mechanically induced self-sustaining reaction, J. Am. Ceram. Soc. 93 (8) (2010) 2252-2256.

[17] V. Bonache, M.D. Salvador, A. Fernández, A. Borrell, Fabrication of full density near-nanostructured cemented carbides by combination of VC/Cr_3C_2 addition and consolidation by SPS and HIP technologies, Int. J. Refract. Met. Hard Mater. 29 (2011) 202-208.

[18] F.W.J. Botta Filho, R. Tomasi, E.M.J.A. Pallone, A.R. Yavari, Nanostrucutured composites obtained by reactive milling, Scr. Mater. 44 (2001) 1735-1740.

[19] A.S.A. Chinelatto, E.M.J.A. Pallone, V. Trombini, R. Tomasi, Influence of heating curve on the sintering of alumina subjected to high-energy milling, Ceram. inter. 34 (2008) 2121-2127.

[20] H. Klung, L. Alexander, X-Ray diffraction procedures. New York: Wiley, 1962.

[21] W.C. Oliver, G.M. Pharr, An improved technique for determining hardness and elastic modulus using load and displacement sensing indentation experiments, J. Mater. Res. 7 (1992) 1564-1583.

[22] K. Niihara, R Morena, D.P.H. Hasselman, Evaluation of K_{IC} of brittle solids by the indentation method with low crack-to-indentation ratios, J. Mater. Sci. Lett. 1 (1982) 13-16.

[23] A.F. Kirstein, R.M. Woolley, Symmetrical bending of thin circular elastic plates on equally spaced point supports, J. Res. Natl. Bur. Stand. C 71 (1967) 1-10.

[24] F.F. Vitman, V.P. Pukh, A method for determining the strength of sheet glass, Zavod Lab 29 (1963) 863-867.

[25] M. Kytiana, J.A. Pask, Formation and control of agglomerates in alumina powder, J. Am. Ceram. Soc. 79 (8) (1996) 2003-2011.

[26] R. Tomasi, A.A. Rabelo, A.S.A. Chinellato, L. Reis, F.W.J. Botta Filho, Characterization of high-energy milled alumina powders, Cerâmica 44 (289) (1998) 166-170.

[27] S. Sumita, W.E. Rhine, K. Bowen, Effects of organics dispersants on the dispersion, packing and sintering of alumina, J. Am. Ceram. Soc. 74 (9) (1991) 2189-2196.

[28] W. Acchar, A.E. Martinelli, F.A. Vieira, C.A.A. Cairo, Sintering behaviour of alumina-tungsten carbide composites, Mater. Sci. Eng. A 284 (2000) 84-87.

[29] R. Marder, C. Estournès, G. Chevallier, R. Chaim, Plasma in spark plasma sintering of ceramic particle compacts, Scr. Mater. 82 (2014) 57-60

[30] Z.H. Zhang, Z.F. Liu, J.F. Lu, X.B. Shen, F.C. Wanga, Y.D. Wang, The sintering mechanism in spark plasma sintering – Proof of the occurrence of spark discharge, Scr. Mater. 81 (2014) 56-59.

[31] W. Acchar, C. Zollfrank, P. Greil, Microstructure of alumina reinforced with tungsten carbide, J. Mater. Sci. 41 (2006) 3299-3302.

[32] S. Bolognini, G. Feusier, D. Mari, T. Viatte, W. Benoit, High temperature mechanical behaviour of Ti(C,N)-Mo-Co cermets, Int. J. Refract. Met. Hard Mater. 16 (1998) 257-268.

[33] L.S. Sigl, H.F. Fischmeister, On the fracture toughness of cemented carbides, Acta Metall. 36 (1988) 887-897.

Figure captions

Figure 1. X-ray diffraction pattern of the powder mixtures after the reaction.

Figure 2. Micrographs of the powders: (a) before and (b) after deagglomeration.

Figure 3. Distribution of the particle size powders: (a) before and (b) after deagglomeration.

Figure 4. Micrographs of fracture surface of the Al_2O_3-5vol.% NbC nanocomposites by conventional sintering at (a) 1550 ºC and (b) 1600 ºC.

Figure 5. Piston speed and displacement during spark plasma sintering of Al_2O_3-5vol.% NbC sample up to 1600 ºC.

Figure 6. Characteristic microstructures of the fracture surface of the Al_2O_3-5vol.% NbC nanocomposites sintered by SPS technique at: (a) 1450 ºC, (b) 1500 ºC, (c) 1550 ºC and (d) 1600 ºC.

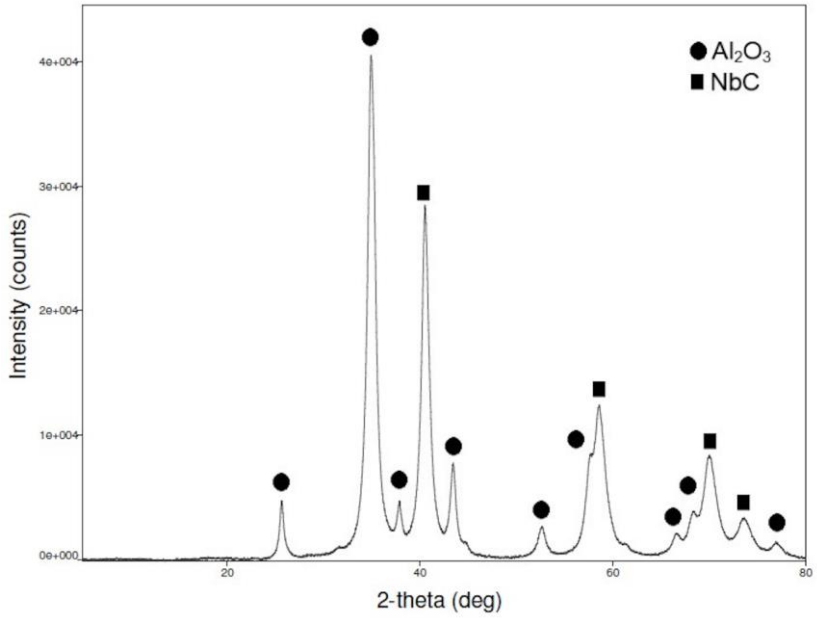

Fig. 1

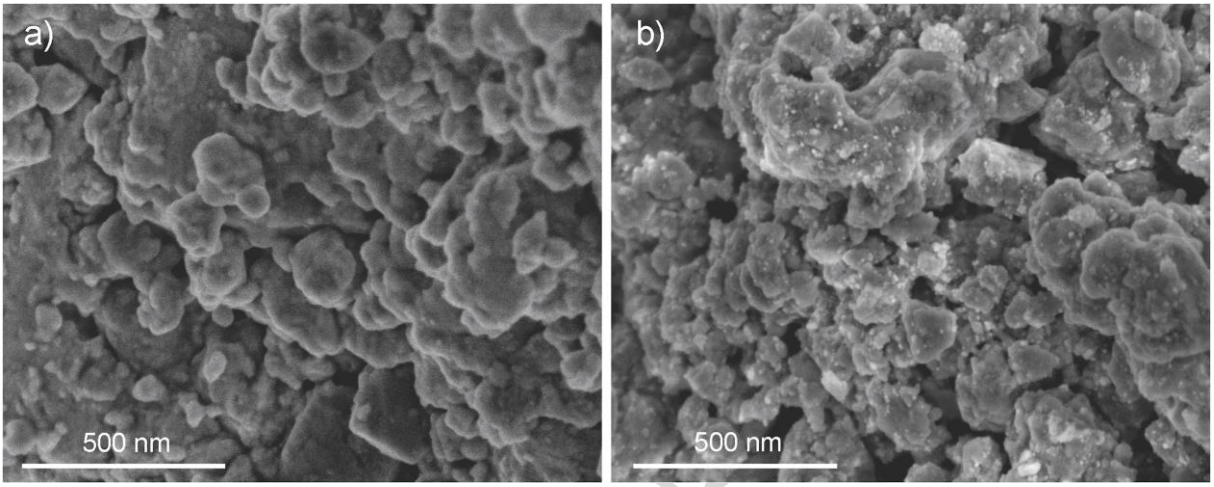

Fig. 2

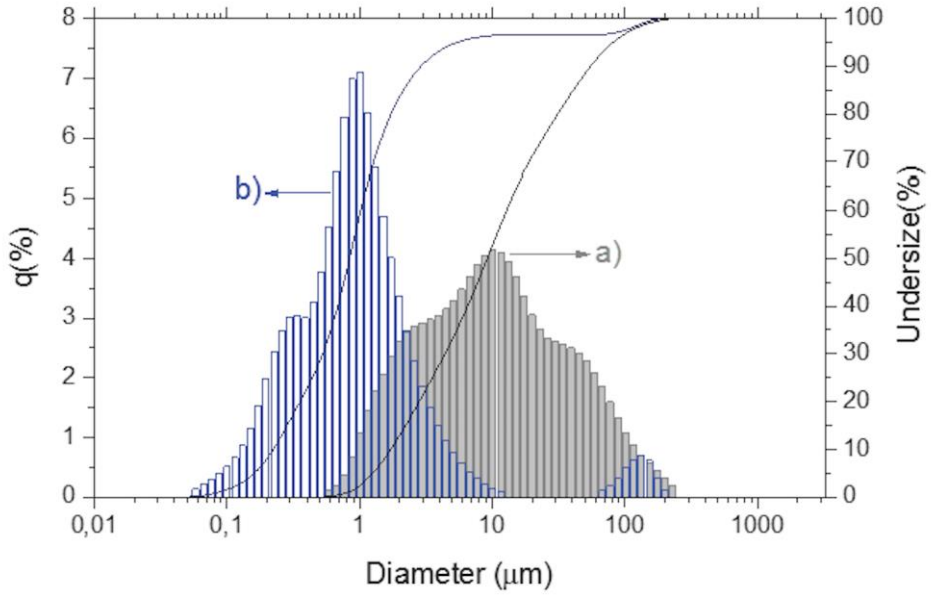

Fig. 3

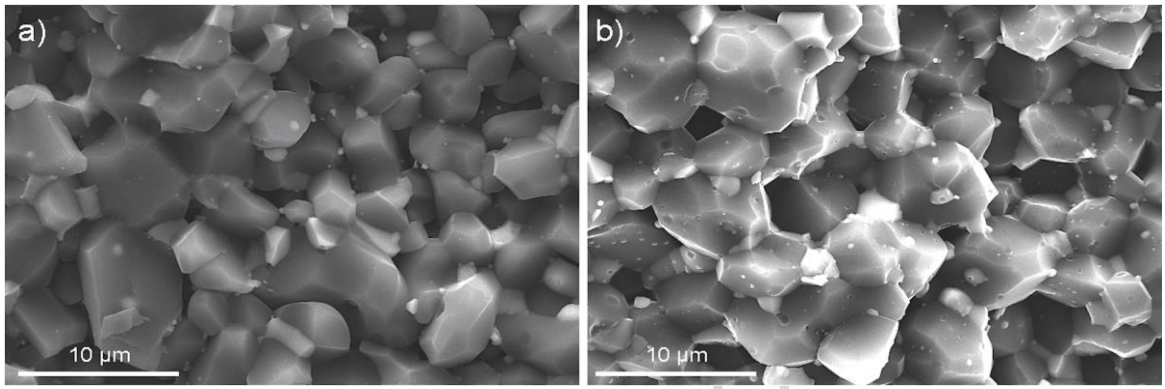

Fig. 4

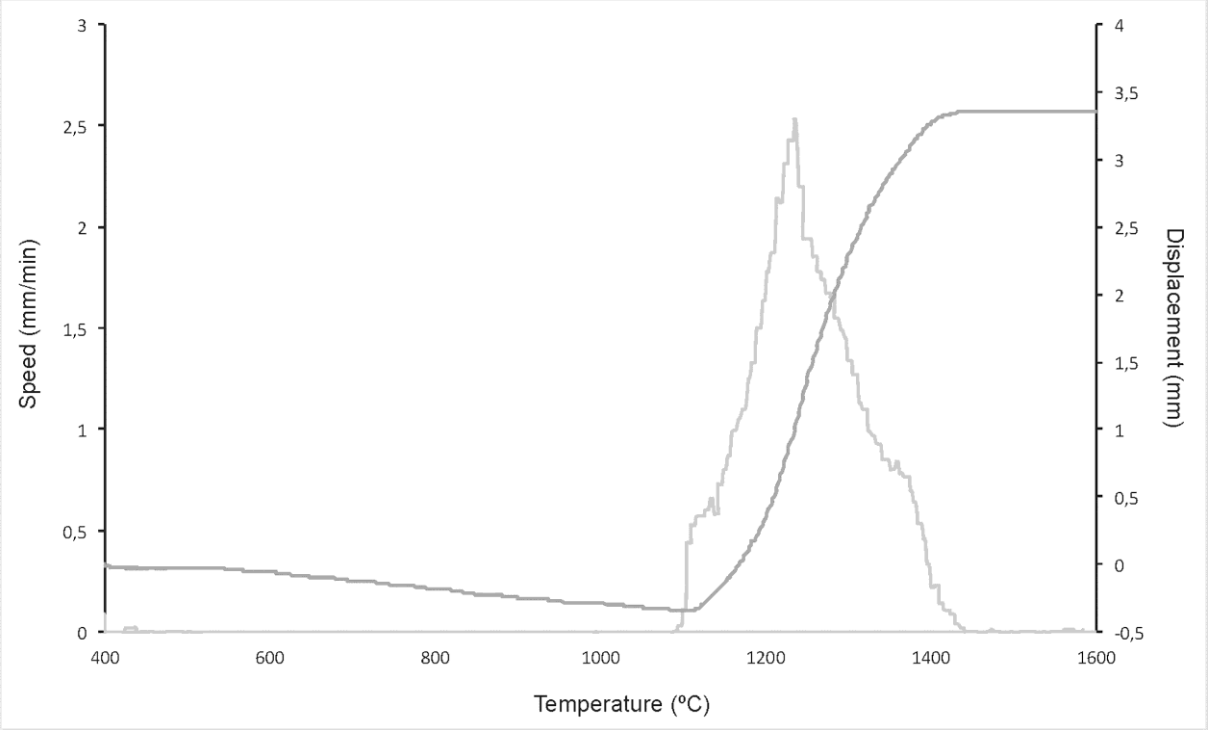

Fig. 5

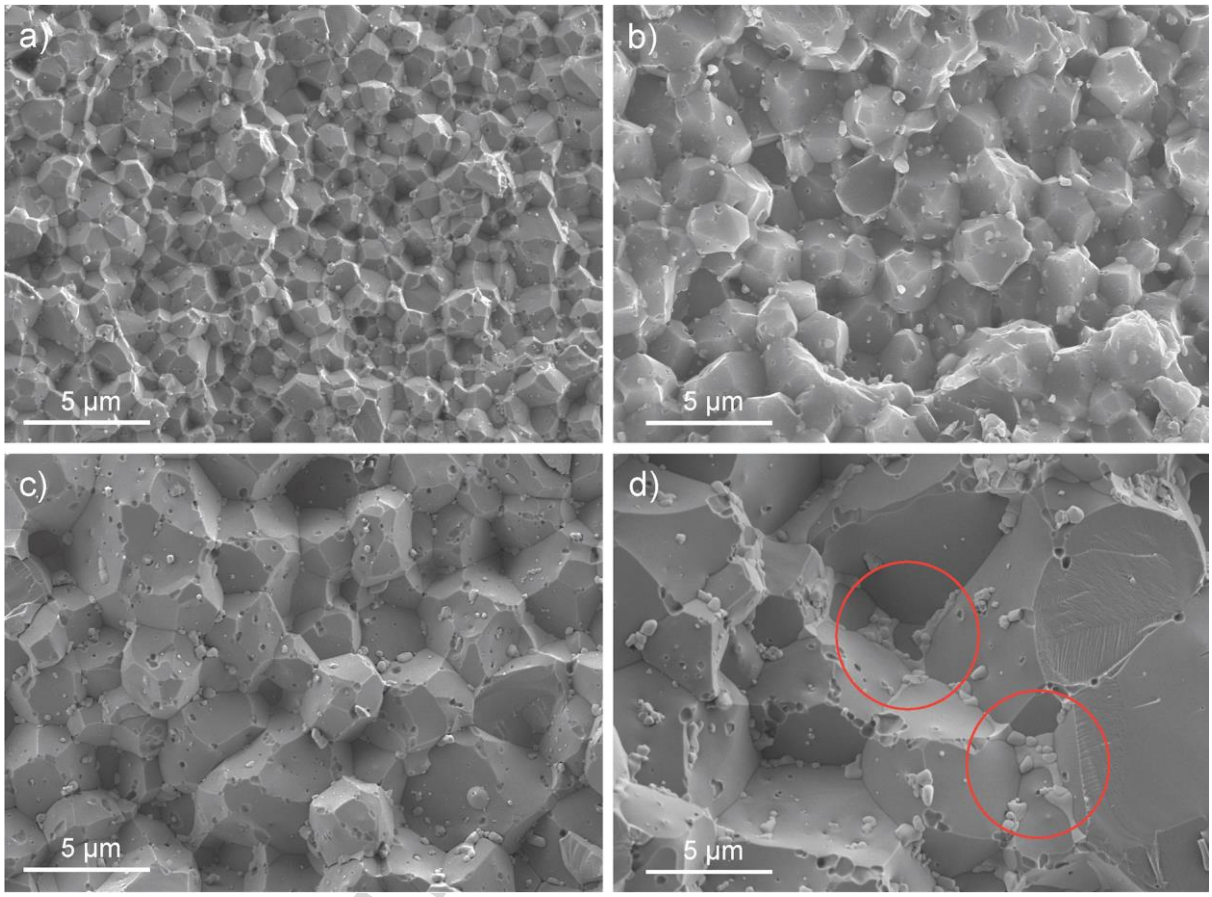

Fig. 6

Highlights

- The effect of NbC second phase as reinforcement of Al_2O_3 nanocomposites is noticeable

- Al_2O_3-NbC nanocomposites obtained by SPS show full density and maximum hardness value

- Samples sintered by SPS show homogeneous distribution of NbC nanoparticles in matrix

- FESEM reveal in sample sintered by SPS at 1600ºC traces of local melting in particles

- The results suggest the possibility of use these materials as cutting tools materials